

Simulation of BOLD Sensitivity of Single-Shot Multi-Echo EPI versus Sample-Induced Susceptibility Gradients

Brice Fernandez¹ and Michael Czisch²

¹Applications and Workflows Europe, GE Healthcare, Munich, Germany, ²Neuroimaging Research Group, Max Planck Institute of Psychiatry, Munich, Germany

Introduction: Standard functional MRI (fMRI) experiments at 3 Tesla use a single echo-time (TE) Echo Planar Imaging (EPI) acquisition, with TE in the range of 30-35 ms and a spatial resolution ranging from 2 to 3.5 mm. This leads to significant distortions¹, loss of signal and BOLD sensitivity² in regions of non-negligible sample-induced susceptibility gradients. In this context, the single shot Multi-echo EPI (MEPI) is known to have several advantages³⁻⁷ over single-echo EPI. Among others, MEPI allows to i) increase fMRI BOLD sensitivity³⁻⁷ ii) acquire a set of T2* weighted images that cover the whole T2* range found in the brain⁸, iii) offer an increased robustness against sample-induced susceptibility gradients³⁻⁵, iv) separate BOLD and non-BOLD components⁷. The use of parallel imaging⁹⁻¹⁰ (PI) is also advantageous for EPI and MEPI to reduce spatial distortion in phase-encoding (PE) direction¹ despite the SNR penalty⁹⁻¹⁰. For MEPI, PI also allows to sample more echoes in a given time window, thus recovering the loss of BOLD sensitivity by the increased number of echoes and the increased BOLD sensitivity of MEPI⁶.

Purpose: The purpose of this work is to determine the theoretical gain and the limit of MEPI in terms of BOLD sensitivity as a function of the sample-induced susceptibility gradients using simulation.

Methods: The derivation follows the development of ref. 2 and uses the BOLD sensitivity (BS) definition of ref. 2. The simulation is similar to the one in ref. 11 but focussing on the above mentioned purpose. Following ref. 2, the image intensity I_n of echo n acquired with a slice thickness Δz , an EPI train with an echo-spacing Δt , an echo time of TE_n and considering a Gaussian slice profile², can be express as a function of susceptibility gradients in slice direction (G^{ssu}) and PE encoding direction (G^{psu}): $I_n \approx \frac{\rho}{Q} \exp\left(-\frac{TE_n}{Q T_2^*}\right) \exp\left(-\left(\gamma G^{ssu} \cdot TE_n \frac{\Delta z}{4\sqrt{\ln(2)}}\right)^2\right)$ with $Q = 1 - \frac{\gamma \Delta t}{2\pi} (\text{FOV}_y) G^{psu}$, ρ the proton density, γ the gyromagnetic ratio, and FOV_y the field of view in the PE direction. Then, the BS of echo n can be written as $BS_n = TE_n I_n / Q$. In the case of MEPI, we consider the following echo combined image⁶: $I_c = \sum_{n=1}^N w_n I_n$ with $w_n = \frac{TE_n I_n}{\sum_{n=1}^N TE_n I_n}$. Using these definitions, it can then be shown that the BS of I_c reduces to $BS_c = \sum_{n=1}^N w_n BS_n$. Additionally, the shifted echo time TE_n/Q due to the gradient susceptibility in the PE direction was taken into account, such as, if the echo is shifted outside the EPI train (or one of the EPI trains in the case of MEPI), the signal and BS is then completely lost² (i.e. signal void). The simulation were made considering a 2 mm isotropic resolution, a net PI acceleration factor of 3, 32 PE blips (when taking the acceleration factor into account), an echo-spacing of 620 μ s with three 3 echoes at TEs of 13, 34, and 56 ms. These parameters were chosen because they are realistic and would represent an acceptable trade-off between spatial resolution, temporal resolution and brain coverage in real-life experiments. Furthermore, two T2* values of 35ms and 66ms that approximately represent the two extreme values found in the brain at 3 Tesla⁸ were considered.

Results: The simulations (figure 1) show the increased robustness of MEPI to susceptibility gradients in terms of BS, particularly against the susceptibility gradient in the slice direction. There is also a substantial gain in robustness to the susceptibility gradient in the PE direction; however it is more modest, particularly when susceptibility gradient in the PE direction is positive and Q become smaller than 1 which led to a complete signal void.

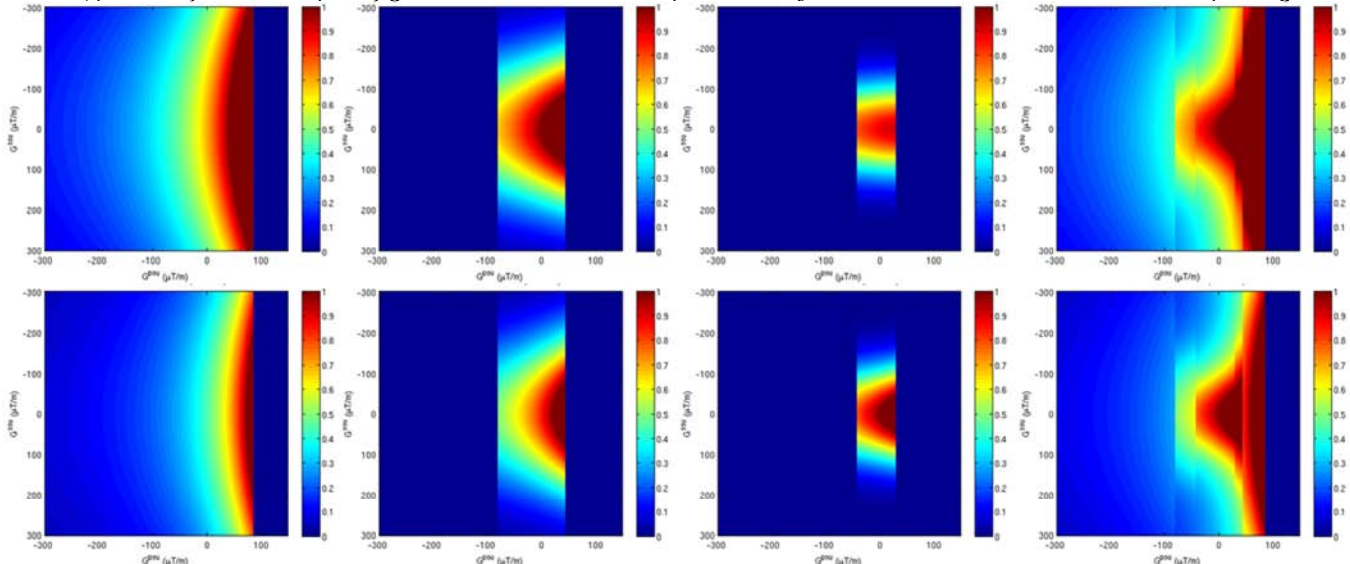


Fig.1: BOLD sensitivity simulation as a function of the susceptibility gradients in the PE direction (G^{psu} , x-axis) and the slice direction (G^{ssu} , y-axis) in $\mu\text{T/m}$ for $T2^*=35\text{ms}$ (row 1) and $T2^*=66\text{ms}$ (row 2). Columns 1, 2 and 3 show the simulated BS of echo 1, 2, and 3 ($TE_n=13, 34$, and 56 ms , respectively). Column 4 shows the simulated BS of the combined image with MEPI. For display purposes, maps were normalised with the maximum BS across TEs when there is no susceptibility gradients ($G^{ssu} = G^{psu} = 0$) for a given $T2^*$ (i.e. for a given row). The display is clipped for values > 1 (i.e. these values are display as 1).

Discussion: The results presented in this work are in accordance with literature³⁻⁶. MEPI offers increased robustness to susceptibility gradients compared to a single echo EPI. The main limitation of MEPI to BS is the susceptibility gradient in PE direction that quickly leads to complete signal void for positive gradients and to significant decrease in BS for negative gradients. It is possible to extend the BS robustness to the susceptibility gradient in PE direction by reducing the acceleration factor (i.e. lengthening the EPI train hence the shifted echo is less likely to fall outside the EPI trains). However, this would lead to an increase of TEs, increased distortions in the PE direction, and/or to a decrease the number of echoes. Our simulation is a simplistic view of the problem, but allows to better understand the limit of MEPI with respect to susceptibility gradients. The main limitation of our simulation is that neither distortion nor SNR loss were taken into account. However, in practice, using a high acceleration factor limits image distortion.

Conclusion: MEPI and its associated echo combination allow for increasing the robustness of fMRI to susceptibility gradients.

References: 1. Koch et al Prog NMR Spectrosc 2009. 2. Deichmann et al. Neuroimage 2002. 3. Posse et al. Neuroimage 2012. 4. Posse et al. MRM 1999. 5. Poser et al. MRM 2006. 6. Bhavas et al. Neuroimage 2013. 7. Kundu et al. Neuroimage 2012. 8. Peters et al. MRI 2007. 9. Pruessmann et al. MRM 1999. 10. Griswold et al. MRM 2002. 11. Domsch et al. MRI 2013.